IEEE Access
Multidisciplinary | Rapid Review | Open Access Journal

Received November 6, 2018, accepted November 16, 2018, date of publication November 20, 2018,
date of current version December 19, 2018.

Digital Object Identifier 10.1109/ACCESS.2018.2882435

Knowledge-Based Crowd Motion for the Unfamiliar Environment

GUIJUAN ZHANG[1,2], DIANJIE LU[1,2], (Member, IEEE), LEI LV[1,2], HUI YU[3], AND HONG LIU[1,2]

[1]School of Information Science and Engineering, Shandong Normal University, Jinan 250358, China
[2]Shandong Provincial Key Laboratory for Novel Distributed Computer Software Technology, Jinan 250358, China
[3]School of Management Science and Engineering, Shandong Normal University, Jinan 250358, China

Corresponding author: Hong Liu (hongliu@sdnu.edu.cn)

This work was supported in part by the National Natural Science Foundation of China under Grant 61572299, Grant 61472232, Grant 61602284, and Grant 61702311, and in part by the Shandong Key Research and Development Program under Grant 2017GSF20105.

ABSTRACT This paper presents a knowledge-based framework for modeling crowd motion in an unfamiliar environment. Three predominant procedures were defined in the framework: knowledge representation, dynamic knowledge transmission, and knowledge-guided wayfinding. First, a semantic-based layered structure is designed to represent knowledge about the unfamiliar environment. Second, to capture important influential factors for knowledge transmission, such as personal influential radius and personal abilities of expressing and assimilating knowledge, we construct a model of personalized knowledge transmission. Third, a probability-based knowledge-guided wayfinding model is presented to produce diverse actions and allow the individuals to adapt to knowledge changes in an unfamiliar environment. Finally, a crowd simulation system is implemented to visualize the analysis in a graphical manner. The proposed method is expected to provide guidance for emergency management especially when the crowd has incomplete knowledge of the environment.

INDEX TERMS Crowd simulation, unfamiliar environment, dynamic knowledge transmission, knowledge-guided wayfinding.

I. INTRODUCTION

Modeling crowd motion is commonly used in emergency evacuations, architectural designs, robotics, traffic dispersion, special effects in games and feature films. A crowd is generally composed of heterogeneous individuals that have various familiarity degrees with the environment. For example, people in a shopping center or an airport may have incomplete knowledge of the area, and their wayfinding behavior is evidently different from those who are familiar with the environment. However, most crowd simulation methods assume that all people are familiar with the environment and can find their way to their goals by an optimal path-searching algorithm [1]–[3]. These emergency evacuation programs are not suitable for the unfamiliar environment since the actual human behaviors are not considered in this situation. Therefore, simulating the motion of a heterogeneous crowd with incomplete knowledge of the environment is necessary in practical applications.

Compared with the in-depth research on simulating crowd motion in familiar environment, only a few studies [4], [5] have been presented to simulate crowd motion in an unfamiliar environment. In these methods, the knowledge are often represented as specific features of the environment, e.g., ''exits list'' [4], ''mental maps'' [5], ''known exits'' [6], etc. These methods assume that the knowledge are transmitted according to the designating rules, and the individuals take the same action under the same conditions. These methods are typical rule-based methods where the rules are carefully designed for specific scenarios, and they are too predictable for more general scenarios.

Modeling crowd motion in an unfamiliar environment is a challenging problem. To study this problem, we consider the features that affect the crowd behaviors in an unfamiliar environment. First, the knowledge representation provides the basis of motion modeling in an unfamiliar environment, and it should describe individual's local view of the unfamiliar environment especially for large and complex scenarios. Second, the knowledge transmission speed among individuals is various because it is influenced by many factors, such as personal influential radius, knowledge attenuation and disturbance due to personal abilities of expressing and assimilating knowledge. Third, the individual action is diverse among

individuals in an unfamiliar environment, and suitable individual action that allow them to adapt to knowledge changes in their local environment should be considered. All of these factors are of critical important for modeling crowd motion in real-world unfamiliar environments. Because the existing methods do not consider these real-world factors, they cannot model and analyze crowd motion in an unfamiliar environment accurately.

This paper presents a knowledge-based simulation framework to model crowd motion in an unfamiliar environment. By studying three predominant procedures (i.e., knowledge representation, dynamic knowledge transmission and knowledge-guided wayfinding) in the framework, our method can model heterogeneous crowd motion realistically in a flexible and controllable way. The proposed method is expected to assist in analyzing crowd behavior in an unfamiliar environment, and developing emergency preplans in this situations. The contributions of this research are listed below.

- A semantic-based layered structure (Semantic-LS) is designed to represent the knowledge about the unfamiliar environment. Semantic-LS is built from the view of human perception, and it can describe individual's local view of the unfamiliar environment effectively.
- A personalized model of knowledge transmission (Personalized-KT) is constructed to capture important influential factors (e.g., personal influential radius, personal abilities of expressing and assimilating knowledge, etc.) on knowledge transmission speed.
- A probability-based knowledge-guided wayfinding model (Probability-KWF) is presented to model the crowd motion in an unfamiliar environment. The model allows the individuals to adapt to knowledge changes in their local environment, and produces diverse actions among individuals in an unfamiliar environment.
- A system is implemented to demonstrate crowd motion in an unfamiliar environment intuitively.

II. RELATED WORK

A. CROWD MODELING METHODS

Simulating the crowd evacuation process has long captivated the attention of researchers. Most of studies focused on how to model the crowd motion, such as Rule-based methods [7], social-force methods [8], [9], and computational intelligent methods [10]. Recently, methods with two steps, global path planning [1] and local collision avoidance [11], were also involved to compute crowd motion in large-scale crowd simulation.

Global path planning often works as the necessary prerequisite for crowd simulation. It computes the static-obstacle-free path towards the goal for each individual. Most global path planning methods abstracted the obstacle-free regions of virtual environment with undirected graph structure [12], [1] and performed search operations on the graph to produce an obstacle-free path for individuals. An undirected graph structure is also used in this paper to represent the static-obstacle-free space. However, we construct the Semantic-LS to process large or complex environment conveniently. Moreover, the Semantic-LS also helps to represent the human knowledge about the environment semantically.

Local collision avoidance methods deals with collision-avoidance with dynamic obstacles and other individuals. These methods can be categorized into two different types: discrete methods and continuum. Researchers often construct motion flow field [13], [14] to compute the collision free path for continuum representation of the crowd, which is suitable for the cases where all individuals have the same goal. However, when individuals have different goals, the methods are expensive to compute their paths. Discrete methods use social force model [15] or geometric-based algorithms [11], [16], [17] to compute collision-free velocities for each individual. Generally, these methods only consider neighboring individuals to reduce computational cost. A typical geometric-based algorithms-reciprocal velocity obstacles (RVO) method [16] is also used in this paper to compute collision avoidance. It can avoid future possible collisions among individuals in velocity space efficiently.

To diversify the crowd motion behaviors, social features are also incorporated into crowd simulation. For example, emotional factors [18], [19], influence of the leadership [6], group behaviors [20], information propagation among crowd [21]–[23], and the influence of overcrowding [24] are considered. However, most of the methods in crowd simulation focus on modeling homogenous crowd where all people are familiar with the environment. Since a crowd may be generally composed of heterogeneous individuals that have various familiarity degrees with the environment, studying the problem of how to model crowd motion in an unfamiliar environment is of great importance in practical applications.

B. CROWD MODELING IN AN UNFAMILIAR ENVIRONMENT

Pelechano and Badler [5] designed a multi-agent system-Maces-to simulate actual human behavior in an unfamiliar environment. Knowledge was represented as mental maps and it could be transmitted among leaders in a room in Maces. Tsai *et al.* [4] designed a multi-agent evacuation simulation system-ESCAPES. The system organizes knowledge as an exit list and transmits it among family members. These two methods are rule-based, and the results are not realistic for more general scenarios because various and complex factors that are important for crowd evacuation have not been considered.

There are also some researches studying crowd social behavior mention the problem of knowledge representation and knowledge transmission incidentally. Most of them endow the individuals with knowledge [6], [23], [25] such as ''known exits'', and ''known routes''. These methods often assume that the optimum path or exit is taken when an individual has enough knowledge. Otherwise, the individual may follow the paths that familiar individuals traveled [6], [23] or

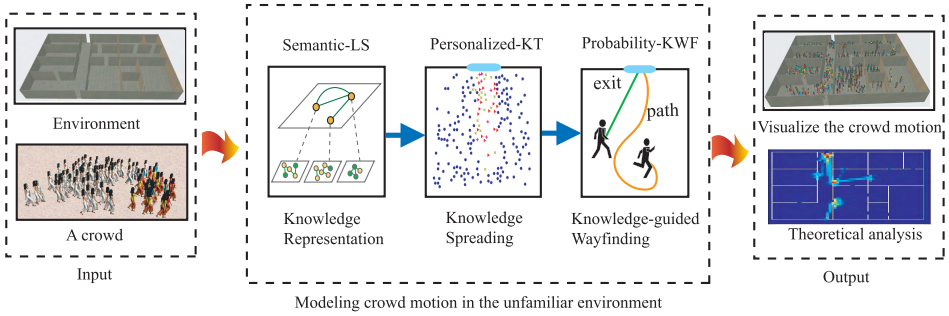

FIGURE 1. Framework of modeling crowd motion in an unfamiliar environment.

run for the exit they used as entrance in an emergency situation [26]. In these methods, everyone follows the same rules and takes the same action even they are different from each other. Therefore, the rule-based methods are too predictable for more general situations.

In this paper, we aim to provide a more flexible and controllable framework to simulate crowd motion in an unfamiliar environment. To the best of our knowledge, no previous work extensively and systematically studies the above problems, which are of great importance in analyzing emergency evacuation in unfamiliar environment.

III. OVERVIEW

Our goal is to simulate actual human wayfinding behavior of a heterogenous crowd with different familiarity in a given unfamiliar environment. The framework presented in this paper includes three predominant procedures: knowledge representation, dynamic knowledge transmission, and knowledge guided wayfinding as shown in Fig. 1. We first design a Semantic-LS to represent the unfamiliar environment from the view of human perceptions. Then, a Personalized-KT model is constructed to model the knowledge transmission which is influenced by important factors (e.g., personal influential radius, and personal abilities of expressing and assimilating knowledge). Next, we present a Probability-KWF model to model individual's diverse actions that adapt to knowledge changes in an unfamiliar environment. Finally, a crowd simulation system is implemented to display the results of our theoretical analysis in a graphical manner. The results can be intuitively understood by non-technical people.

The framework is defined formally as follows. Let $\mathcal{F} = (\mathcal{I}, \mathcal{MC}, \mathcal{O})$ be the framework, where $\mathcal{I} = (\mathcal{M}, P)$ is the input, $\mathcal{O}$ is the output, and $\mathcal{MC}$ computes the crowd motion in unfamiliar environment. As for the input, $\mathcal{M}$ is the 3D model of the environment and $P = (N, \boldsymbol{X}, \mathcal{V}, \boldsymbol{G})$ denotes a crowd with N individuals that have position $\boldsymbol{X}$, speed $\mathcal{V}$ and goal position $\boldsymbol{G}$ initially. As for the motion computation $\mathcal{MC} = \{(\mathcal{KR}, \mathcal{KD}, \mathcal{KW}, \mathcal{CA})|A\}$, $A = (\boldsymbol{x}, v, \boldsymbol{g}, \varepsilon, \varrho, R)$ is an individual in the crowd, where $\boldsymbol{x}$ is the position, v is speed, $\boldsymbol{g}$ is goal position, ε and ϱ is the ability of knowledge expression and assimilating knowledge respectively, and R is personal influential radius. The four tuples $(\mathcal{KR}, \mathcal{KD}, \mathcal{KW}, \mathcal{CA})$ defines the operations on each individuals. $\mathcal{KR}$ is the operation of knowledge representation that enables the knowledge to be perceived and learned by individuals; $\mathcal{KD}$ is the operation of dynamic knowledge transmission which describes the information gain of each individual during simulation; $\mathcal{KW}$ is the operation of knowledge-guided wayfinding operation that finds a specific route for each individual; and $\mathcal{CA}$ is the collision avoidance procedure that computes the collision-free velocity of each individual.

IV. KNOWLEDGE REPRESENTATION

Generally, the most intuitive representation of knowledge is a specific route for each individual. However, a number of paths are available for an individual in a scenario, which presents a great challenge to storing resources, and limiting the scalability and efficiency of crowd simulation method significantly.

We represent the knowledge from the view of human perception to simplify the problem. A semantic-LS $\mathcal{KR}$ is presented here. To indicate the familiarity of an individual with an unfamiliar environment and compute the detailed path, $\mathcal{KR}$ includes three layers, base knowledge $\mathcal{K}_b$ representing the topological and geometrical information semantically in the bottom layer, individual knowledge $\mathcal{K}$ denoting familiar degree in the middle layer, and specific knowledge $\mathcal{K}_s$ expressing the navigation path in the top layer.

A. BASE KNOWLEDGE $\mathcal{K}_b$

Base knowledge $\mathcal{K}_b$ is a layered structure that abstracts the topological and geometrical information of $\mathcal{M}$ semantically; it can be shared by all individuals located in $\mathcal{M}$. Observe that our perception (vision and hearing system) of the environment often works in a local area, we first divide the 2D domain of $\mathcal{M}$ into perception-reachable subregions geometrically, and then detail the description of each subregion. A layered graph $\mathcal{G}$, named region graph, is used to express $\mathcal{K}_b$.

1) REGION SUBDIVISION

Let $\mathbb{C}$ be the 2D projection of the 3D environment model $\mathcal{M}$. $\mathbb{C}$ denotes the simulation domain that is encompassed by the axis-aligned bounding box of the projected model. $\mathbb{C}$ is divided into a set of subregions $\mathbb{C} = \{c_i\}$, where each

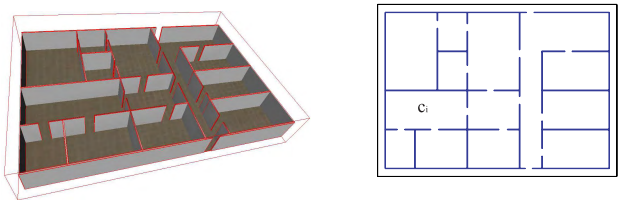

FIGURE 2. Extracting information from the 3D environment. (a) the 3D environmental model with the obstacles, and the bounding box is highlighted by red lines. (b) the 2D projected model. $\mathcal{C}$ is the area enclosed by border lines, and each subregion of $\mathcal{C}$ is a single room in this example.

subregion c_i is an axis-aligned box and $\mathbb{C} = \bigcup c_i$. For example, in Fig. 2(a), the 3D environment model $\mathcal{M}$ is provided. Fig. 2(b) shows the 2D projected model. $\mathbb{C}$ is the area enclosed by border lines, and each subregion of $\mathbb{C}$ is a single room in the example. The subdivision process can be executed efficiently and intuitively because daily large-scale scenes are often managed by different subsections. The subdivision is executed according to the following principles.

Functional principle: The region is divided into subregions according to different functions. For example, a super market is often divided into different sections, such as fruits, vegetables, dairy, etc.

Geometrical principle: Geometrical shape is the most apparent feature for subdivision. Geometric information such as regular shape, symmetry, and similarity, as well as semi-closeness is regarded as the references of the region subdivision.

Size principle: Each subregion has at least one exit. The smallest subregion is a semi-closed space, such as a room.

2) REGION-GRAPH CONSTRUCTION

The region graph is defined in this paper as, but not limited to, a two-layer graph $\mathcal{G}(\mathbb{C}(V, E), \mathcal{L})$. The top layer of $\mathcal{G}$ describes the subregions $\mathbb{C} = \{c_i\}$ and their connections $\mathcal{L}$. Each subregion $c_i \in \mathbb{C}$ in the bottom layer is extended to a graph to describe the geometrical and topological features of c_i thoroughly.

Each subregion $c_i \in \mathcal{C}$ is a vertex of the top-layer graph. Given two adjacent subregions c_i and c_j ($i < j$), the center point $\boldsymbol{O}_k$ of each exit on the shared edge of c_i and c_j is obtained. Thus, the connection nodes of c_i and c_j is $link(c_i, c_j) = \{\boldsymbol{O}_1, \cdots, \boldsymbol{O}_m\}$. The edges $\mathcal{L}$ of the top-layer graph is obtained by creating $\| link(c_i, c_j) \|$ edges, and each edge $\mathcal{L}_{ij}(\boldsymbol{O}_k)$ denotes that c_i and c_j are connected by an exit located at $\boldsymbol{O}_k$.

The bottom layer $\mathbb{C}(V, E) = \{c_i(V, E)\}$ of $\mathcal{G}$ expresses the geometrical and topological information of each subregion c_i. The roadmap $R_i(V, E)$ is used to represent $c_i(V, E)$. $R_i(V, E)$ can be effectively constructed with the probabilistic-based method [27]. The vertices V of $R_i(V, E)$ are generated randomly in the obstacle-free space of the subregion. Adjacent nodes that are mutually visible and lie within a threshold distance of each other are connected by an edge $e \in E$.

The connection nodes are added to the roadmap of the corresponding subregions to ensure that the roadmaps of all reachable subregions can be extended into a large connected graph. The edges between the connection points and their visible adjacent vertices in the roadmap are also created accordingly. Fig. 3 shows an example.

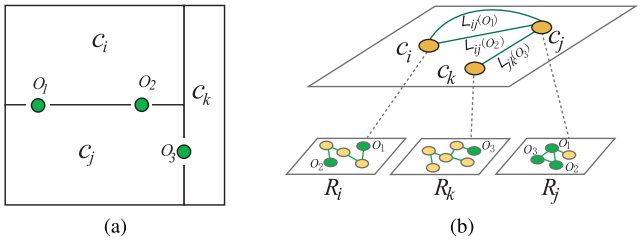

FIGURE 3. An example of creating a region graph. (a) 2D projection of the virtual environment. c_i and c_j are connected by two exits with the center points O_1 and O_2. So $link(c_i, c_j) = \{O_1, O_2\}$. Similarly, $link(c_j, c_k) = \{O_3\}$ and $link(c_i, c_k) = \emptyset$. (b) structure of the region graph. The top layer denotes the connections among c_i, c_j and c_k. The corresponding three edges $\mathcal{L}_{ij}(O_1)$, $\mathcal{L}_{ij}(O_2)$ and $\mathcal{L}_{jk}(O_3)$ are shown. The bottom layer describes each subregion with a roadmap. O_1, O_2 and O_3 are added to the roadmaps R_i, R_j, and R_k.

B. INDIVIDUAL KNOWLEDGE $\mathcal{K}$

Individual knowledge denotes the familiarity degree of each individual. For the top layer of region graph $\mathcal{G}$, we define a vector $\mathcal{K}_i = \{k_i^1, \cdots, k_i^s\}$ with each component $k_i^j \in [0, 1]$ indicates the familiarity of c_j for individual i. A larger value means that the individual is more familiar with the subsection. The individual is called an expert if $k_i^j = 1$, and a novice if $k_i^j = 0$ in subregion c_j. In addition, the individual is called an knowledgeable person if $k_i^j \geq 0.5$ in c_j. We use $N(k_i^j = 1)$, $N(k_i^j = 0)$, and $N(k_i^j \geq 0.5)$ to represent the number of experts, novices, and knowledgeable person in c_j.

C. SPECIFIC KNOWLEDGE $\mathcal{K}_s$

Specific knowledge is defined as an available path $\mathcal{P}$ from the start to the goal position of an individual. All vertices and edges on the path are obtained from the bottom layer of the region graph $\mathcal{G}$. $\mathcal{K}_s$ can be computed conveniently using base knowledge $\mathcal{K}_b$ and individual knowledge $\mathcal{K}$ according to our wayfinding algorithm, which will be introduced in next Section.

Our method can process the large and complex environment incrementally, and construct the more general structure-$\mathcal{G}$ which describes the topological and geometrical information of the environment automatically. The available path for each individual obtained based on Semantic-LS without considering the trivial details. Furthermore, the familiarity settings of the population is more realistic by defining the individual knowledge as a continuous value between 0 and 1 rather than a discrete value 0 or 1 as in existing methods. It enable us to express the intermediate states of familiarity.

V. KNOWLEDGE TRANSMISSION

When people have incomplete knowledge of an area, they may communicate with her neighbors to obtain more information. However, this process is influenced by many important factors, such as personal influential radius and personal abilities of expressing and assimilating knowledge. We propose personalized-KT model in this section. During knowledge transmission process, the individual knowledge $\mathcal{K}_i$ increases dynamically when individual i obtains more information from other knowledgeable individuals.

In order to study the changes of knowledge with time, we suppose that time is slotted into equal intervals. Knowledge is periodically updated for each interval and remains unchanged during a time slot. Given the individual knowledge of individuals i in the nth time step, our goal is to compute its individual knowledge in the $(n+1)$th time step as $\mathcal{K}_i^{n+1} = \mathcal{KD}(\mathcal{K}_i^n)$. At each time step n, an individual i communicates with its more knowledgeable neighbors. Let vector $\widetilde{\mathcal{K}}_i = \{\tilde{k}_i^1, \cdots, \tilde{k}_i^s\}$ be the knowledge obtained from its neighbors, which is defined as

$$\tilde{k}_i^j = \begin{cases} \underset{m \in \mathcal{N}_i}{argmax}\ \varepsilon_m \varrho_i (k_m^j - k_i^j) & \text{if } k_m^j > k_i^j \\ 0 & \text{otherwise.} \end{cases} \tag{1}$$

Equation (1) indicates that the individual tries to obtain the maximum level of knowledge from its neighbors. In this equation, $\mathcal{N}_i$ is the neighbor set of the individual i, ε_m is the personal ability of knowledge expression for individual m, and ϱ_i is personal ability of knowledge assimilation for individual i.

In equation (1), a neighbor $j \in \mathcal{N}_i$ is an individual that the distance between i and j is smaller than a threshold R_i and that there is no obstacle blocking the sight line between i and j, allowing knowledge to be transmitted through communication, gestures or facial expressions. Here, R_i is the personal influential radius of i, and it controls the speed of knowledge spreading.

Considering that both the personal abilities of expressing and assimilating knowledge are various among individuals, they are numerically formalized by numbers drawn from a specified probability distribution. We suppose that both ε_i and ϱ_i are subject to normal distribution $\mathcal{N}(\mu, \sigma^2)$. Thus, ε_i and ϱ_i can be represented as

$$\varepsilon_i = \mathcal{N}(\mu_\varepsilon, \sigma_\varepsilon^2), \quad \varrho_i = \mathcal{N}(\mu_\varrho, \sigma_\varrho^2). \tag{2}$$

Both ε_i and ρ_i are random numbers between [0, 1]. Larger values mean stronger abilities of expressing or assimilating knowledge. For example, a larger ϱ_i implies that individual i is more outgoing in obtaining useful information, whereas a smaller ϱ_i implies that the individual is more shy in communicating with others. The two parameters ε_i and ρ_i also control the attenuation and disturbance of knowledge during spreading process. Larger values of the two parameters produce less attenuation and disturbance, according to Equation (1).

Finally, the individual knowledge of i can be updated according to

$$\mathcal{K}_i^{n+1} = \mathcal{K}_i^n + \widetilde{\mathcal{K}}_i. \tag{3}$$

After updating individual knowledge $\mathcal{K}_i^{n+1}$, specific knowledge $\mathcal{K}_s$ is also updated accordingly. Each individual re-selects a specific route $\mathcal{P}$. The individual has more opportunities to select an optimal path when $\mathcal{K}_i$ increases.

VI. KNOWLEDGE-GUIDED WAYFINDING

To get the path $\mathcal{P}$ from specific knowledge $\mathcal{K}_s$ of each individual, a Probability-KWF model is developed in this section. It can produce diverse individual actions that adapt to knowledge changes in an unfamiliar environment. In Probability-KWF model, we obtain the vertices and edges of the specific route $\mathcal{P}$ in two phases: high-level and low-level navigation. High-level navigation determines the vertices on the path that connect different subregions while low-level navigation computes the vertices and edges within a subregion.

A. HIGH-LEVEL NAVIGATION

The high-level navigation is executed in four steps, which are as follows.

Step 1 (Computing the Selection Probability): First, two sets $\mathcal{C}_{neighbors}$ and $\mathcal{C}_{cand}$ are constructed. Let c_{cur} be the subregion where i is located currently. $\mathcal{C}_{neighbors}$ is the neighborhood subregions of c_{cur}. $\mathcal{C}_{cand}$ is a candidate set that contains all subregions that have at least one path to the destination. Thus, $\mathcal{C}_{cand} \subseteq \mathcal{C}_{neighbors}$. To obtain $\mathcal{C}_{cand}$, all available paths $\mathbb{P}$ from the start subregion c_s to the goal subregion c_g of individual i on the top layer of $\mathcal{G}(\mathbb{C}(V, E), \mathcal{L})$ are computed using a backtracking algorithm combined with depth-first search mechanism on the top layer of $\mathcal{G}(\mathbb{C}(V, E), \mathcal{L})$ conveniently. Then, $\mathcal{C}_{cand}$ is constructed by selecting all subregions that next to c_{cur} in each path of $\mathbb{P}$.

Second, the selection probability for each subregion in $\mathcal{C}_{neighbors}$ is computed. Let $p(i, j)$ be the selection probability of subregion c_j in $\mathcal{C}_{neighbors}$ for each individual i. To ensure that the individual does not consider the familiar subregion which does not have a path to the destination according to observation 2, we set $p(i, j) = 0$ if $c_j \in \mathcal{C}_{neighbors} \backslash \mathcal{C}_{cand}$ and $k_i^j \geq \vartheta$ where ϑ is a threshold. However, the unfamiliar subregions that do not have a path to the destination can still be selected. Thus, if $k_i^j < \vartheta$, $c_j \in \mathcal{C}_{neighbors} \backslash \mathcal{C}_{cand}$ will be added to $\mathcal{C}_{cand}$.

Third, the selection probability $p(i, j)$ for subregion $c_j \in \mathcal{C}_{cand}$ is calculated as

$$p(i, j) = \begin{cases} k_i^j / \sum k_i^j & \text{if } \sum k_i^j > 0 \\ 1 / \parallel \mathcal{C}_{cand} \parallel & \text{else,} \end{cases} \tag{4}$$

where $\parallel \cdot \parallel$ is the size of the set. In Equation (4), a larger k_i^j yields higher selection probability. When all subregions are strange places for i (i.e., $\sum k_i^j = 0$), random sampling is used.

Step 2 (Adjusting the Selection Probability): The selection probability $p(i, j)$ of subregion $c_j \in \mathcal{C}_{cand}$ should be adjusted

because individuals tend to find the optimal path when they are familiar with the environment. Suppose that individual i is familiar with subregion c_j if $k_i^j \geq \vartheta$. Thus, a set with familiar subregions $\mathcal{C}_f$ for i is easily obtained by adding $c_j \in \mathcal{C}_{cand}$ which satisfies $k_i^j \geq \vartheta$ to $\mathcal{C}_f$ intuitively. Then, a subset $\mathcal{C}_{short} \subset \mathcal{C}_f$ that contains the subregions that have shortest path distance from c_{cur} to c_g is constructed. Finally, the selection probability $p(i,j)$ of $c_j \in \mathcal{C}_{cand}$ is adjusted as

$$p(i,j) = \begin{cases} p(i,j) + \lambda \sum\limits_{c_k \in \mathcal{C}_{cand} \setminus \mathcal{C}_{short}} p(i,k) & \text{if } c_j \in \mathcal{C}_{short} \\ (1 - \lambda \parallel \mathcal{C}_{short} \parallel) p(i,j) & \text{else,} \end{cases} \tag{5}$$

where $0 \leq \lambda \leq 1/ \parallel \mathcal{C}_{short} \parallel$ controls the eagerness of an individual in selecting the shortest path. Evidently, a large λ means that the individual is more inclined to select the subregion that is nearest to the goal region.

Step 3 (Selecting a Subregion): Given an array of the selection probability $p(i,j)$, the roulette wheel selection method [28]–[30] is used to obtain the next subregion c_{next}. Specifically, the cumulative probability is computed to make each candidate subregion c_j lie in $(P_s(i,j), P_e(i,j)]$, where

$$P_s(i,j) = \sum_{\substack{c_k \in \mathcal{C}_{cand} \\ k<j}} p(i,k), \quad P_e(i,j) = \sum_{\substack{c_k \in \mathcal{C}_{cand} \\ k<j+1}} p(i,k).$$

A higher selection probability yields a larger interval, which means that the subregion with a larger $p(i,j)$ is more likely to be selected. Then, a uniform(0,1) random number $\wp$ is generated. If $P_s(i,j) < \wp \leq P_e(i,j)$, c_j will be selected as the next subregion $c_{next} = c_j$. This selection process will be repeated until a subregion c_{next} that has not been visited by i before is found.

Step 4 (Adding the Connection Node to $\mathcal{P}$): The nearest connection node $\boldsymbol{O}_m \in link(c_{cur}, c_{next})$ is added to the specific route $\mathcal{P}$ after computing c_{next} for individual i, where

$$\boldsymbol{O}_m = \underset{\boldsymbol{O}_k \in link(c_{cur}, c_{next})}{argmin} \widehat{\|\boldsymbol{O}_k - \boldsymbol{x}_i\|}. \tag{6}$$

$\boldsymbol{x}_i$ is the position of individual i; $\widehat{\|\boldsymbol{O}_k - \boldsymbol{x}_i\|}$ denotes the path distance between $\boldsymbol{O}_k$ and $\boldsymbol{x}_i$.

B. LOW-LEVEL NAVIGATION

Low-level navigation computes the path from $\boldsymbol{x}_i$ to the subgoal in c_{cur}. Two steps are involved in this process.

Step 1 (Determining the Subgoal $\tilde{\boldsymbol{g}}_i$): Check whether individual i has achieved its target subregion c_g. If so, subgoal $\tilde{\boldsymbol{g}}_i$ is set to the goal position g_i of individual i. Otherwise, $\tilde{\boldsymbol{g}}_i$ is set as the nearest connection node $\boldsymbol{O}_m$ denoted in Equation (6).

Step 2 (Computing the Path From $\boldsymbol{x}_i$ to $\tilde{\boldsymbol{g}}_i$): Subgoal $\tilde{\boldsymbol{g}}_i$ is visible to individual i if obstacles do not exits between $\tilde{\boldsymbol{g}}_i$ and $\boldsymbol{x}_i$, and the distance between $\tilde{\boldsymbol{g}}_i$ and $\boldsymbol{x}_i$ is smaller than the visual range R_i of individual i. In this case, the shortest path on $R_{cur}(V,E)$ from $\boldsymbol{x}_i$ to $\tilde{\boldsymbol{g}}_i$ is directly added to the specific route $\mathcal{P}$.

If $\tilde{\boldsymbol{g}}_i$ is not visible, we suppose that the probability of selecting the shortest path is proportional to its knowledge, that is, $\tilde{p}_i \propto k_i^{cur}$. Here, $\tilde{p}_i = ak_i^{cur} + b$, where $a > 0$, $b \geq 0$ and $a + b \leq 1$. The roulette wheel selection method is applied after calculating $\tilde{p}_i$ for each individual to get the path from $\boldsymbol{x}_i$ to $\tilde{\boldsymbol{g}}_i$.

Specifically, we first add $\boldsymbol{x}_i$ to the roadmap $R_{cur}(V,E)$ of the bottom layer of $\mathcal{G}$. $\boldsymbol{x}_i$ is connected to the visible vertices on $R_{cur}(V,E)$. Then, a uniform (0,1) random number $\wp$ is generated and compared with $\tilde{p}_i$. If $\wp \leq \tilde{p}_i$, the shortest path on $R_{cur}(V,E)$ from $\boldsymbol{x}_i$ to $\tilde{\boldsymbol{g}}_i$ is selected. Otherwise, a DFS algorithm is involved to get a path from $\boldsymbol{x}_i$ to $\tilde{\boldsymbol{g}}_i$. To offer a wider variety of paths for the crowd, we randomly select the next vertex which is adjacent to current vertex.

Algorithm 1 *Wayfinding*(c_{cur}, i)

Input: $\mathcal{G}$,$\mathcal{K}_i$,c_{cur},c_g
Output: $\mathcal{P}$, c_{next}
begin
  mark(c_{cur});
  if $c_{cur} = c_g$ **then**
    $\mathcal{P} \longleftarrow \mathcal{P} \cup Findpath(\boldsymbol{g}_i, \boldsymbol{x}_i, k_i^{cur})$;
    return;
  for *each* $c_j \in \mathcal{C}_{cand}$ **do**
    $p(i,j) \longleftarrow ComputeProbability(\mathcal{K}_i, \mathcal{C}_{cand})$;
  repeat
    $c_{next} \longleftarrow Select(\mathcal{C}_{cand}, p)$;
  until c_{next} *is unmarked*;
  $O_m \longleftarrow NearestConnectionPoint(c_{cur}, c_{next})$;
  $\mathcal{P} \longleftarrow \mathcal{P} \cup Findpath(\boldsymbol{O}_m, \boldsymbol{x}_i, k_i^{cur})$;

Algorithm 1 shows the wayfinding process of each individual. In the algorithm, *mark*$(\cdot)$ adds the marker for the subregion that has been visited before. *ComputeProbability*$(\cdot)$ calculates $p(i,j)$ according to Step 1 and 2 in the high-level navigation process. *Select*$(\cdot)$ returns the subregion c_{next} using Step 3 in the high-level navigation process. This process is repeated until a subregion c_{next} that has not been visited before is found. *Findpath*$(\cdot)$ obtains a path for individual i that moves from $\boldsymbol{x}_i$ to $\tilde{\boldsymbol{g}}_i$ according to the two steps of low-level navigation. The algorithm is essentially a DFS process on the top layer of the region graph $\mathcal{G}$ with the only difference that the subregions have priority to be selected.

VII. SYSTEM IMPLEMENTATION

We implement a simulation system to visualize the theoretical analysis in a graphical manner. Our system is built upon the typical crowd simulation system [16]. To model the crowd motion in unfamiliar environment, we need to compute the preferred velocity (static-obstacle-free velocity) and collision-free velocity for each individual. After obtaining the velocity, the position and knowledge of individual are updated. The implementation details are outlined in Algorithm 2.

Algorithm 2 Crowd Simulation in Unfamiliar Environment

Input: $\mathcal{M}$, time step Δt, number of individuals N
Output: A sequence of simulation results
begin
  $n \longleftarrow 0$;
  $\mathcal{G}(\mathbb{C}(V, E), \mathcal{L}) \longleftarrow RegionGraph(\mathcal{M})$;
  $(P^n, \mathcal{K}^n) \longleftarrow Initialization(\mathcal{G}, N)$;
  for *each individual* **do**
    $c_{cur} = c_{next} = c_s$;
  while $\exists$ *individual NOT reach its goal* **do**
    for *i Not reach* $\boldsymbol{g}_i$ **do**
      $c_{cur} \longleftarrow InWhichSubregion(\boldsymbol{x}_i^n, \mathcal{G})$;
      if $c_{cur} = c_{next}$ **then**
        $(\mathcal{P}, c_{next}) \longleftarrow Wayfinding(c_{cur}, i)$;
      $\tilde{\boldsymbol{v}} \longleftarrow ComputePreferV(c_{cur}, \boldsymbol{x}_i, \mathcal{P})$;
      $\boldsymbol{v}_i \longleftarrow CollisionAvoidance(\tilde{\boldsymbol{v}}_i)$;
      $\boldsymbol{x}_i^{n+1} \longleftarrow \boldsymbol{x}_i^n + \Delta t \boldsymbol{v}_i$;
    for *i has reached* $\boldsymbol{g}_i$ **do**
      stay near $\boldsymbol{g}_i$;
    $\mathcal{K}_i^{n+1} \longleftarrow UpdateKnowledge(\mathcal{K}_i^n, \boldsymbol{x}^{n+1})$;
    $n \longleftarrow n + 1$;

1) INITIALIZATION

Given the region graph $\mathcal{G}(\mathbb{C}(V, E), \mathcal{L})$, $Initialization(\cdot)$ generates N individuals in the obstacle-free regions. The start position $\boldsymbol{x}_i^0$ and goal position $\boldsymbol{g}_i$ of individual i can be obtained from random sampling. $\boldsymbol{g}_i$ can also be set as a specified location (i.e., building exit) if necessary. In this algorithm, the knowledge $\mathcal{K}$ of the crowd can be initialized according to normal distribution $N(\mu, \sigma^2)$. The knowledge can also be extended to other distributions as necessary.

2) COMPUTING THE PREFERRED VELOCITY $\tilde{v}_i$

Procedure $ComputePreferV(\cdot)$ computes the preferred velocity $\tilde{\boldsymbol{v}}_i$ of each individual. Here, the preferred velocity is static-obstacle-free that leads individual i toward goal position $\boldsymbol{g}_i$. Computing $\tilde{\boldsymbol{v}}_i$ involves two steps in our method. First, the magnitude v of $\tilde{\boldsymbol{v}}_i$ is initialized in a fixed-interval $[v_{min}, v_{max}]$. Second, the direction $\boldsymbol{d}$ of $\tilde{\boldsymbol{v}}_i$ is determined. Given the $\mathcal{P}$ from specific knowledge, we find a vertex v_o to steer the motion of individual i. v_o is the vertex visible to $\boldsymbol{x}_i$ and has a minimum path distance to goal position $\boldsymbol{g}_i$. Motion direction is set as $\boldsymbol{d}_i = v_o - \boldsymbol{x}_i$. Thus, the preferred velocity of individual i is $\tilde{\boldsymbol{v}}_i = v\boldsymbol{d}_i$.

Preferred velocity $\tilde{\boldsymbol{v}}_i$ is affected by the specific knowledge $\mathcal{P}$ of the individual, which is different from traditional methods. More knowledge yields a larger probability to move along the shortest path.

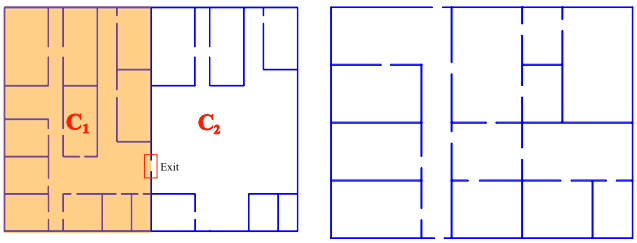

FIGURE 4. Two scenarios used in the experiments. (a) A scenario with two subregions c_1 and c_2. (b) A scenario with each single room is a subregion.

3) LOCAL COLLISION AVOIDANCE

$CollisionAvoidance(\cdot)$ computes the collision-free velocity of an individual given the preferred velocity $\tilde{\boldsymbol{v}}_i$. $\tilde{\boldsymbol{v}}_i$ only avoids static obstacles in a scenario, whereas $\boldsymbol{v}_i$ can avoid dynamic obstacles or other individuals in the scenario. RVO [16] which is the most popular local collision avoidance method for crowd simulation is used. Crowd collision avoidance based on RVO method is executed in the following two steps.

First, all possible velocities of individual i that lead to a potential collision with the other individual j in the neighborhood are computed. These velocities are represented by the reciprocal velocity obstacle

$$RVO_j^i = \{\boldsymbol{v}_i' | \lambda(\boldsymbol{x}_i, 2\boldsymbol{v}_i' - \boldsymbol{v}_i - \boldsymbol{v}_j) \cap gs_j \oplus -gs_i \neq \emptyset\},$$

where gs_i is the geometric shape of individual i, $\lambda(\boldsymbol{x}, \boldsymbol{v})$ is the ray shot from $\boldsymbol{x}$ in the direction of $\boldsymbol{v}$. $gs_j \oplus gs_i$ is the Minkowski sum of the two sets gs_j and gs_i, i.e. $gs_j \oplus gs_i = \{\boldsymbol{x}_i + \boldsymbol{x}_j | \boldsymbol{x}_i \in gs_i, \boldsymbol{x}_j \in gs_j\}$. $-gs_i$ is the geometric shape gs_i reflected in its reference point, i.e., $-gs_i = \{-\boldsymbol{x}_i | \boldsymbol{x}_i \in gs_i\}$. RVO_j^i represents all possible velocities that make i collision with j potentially. Therefore, admissible velocities that is collision-free and oscillation-free can be obtained easily by choosing the velocities of individual i outside of RVO_j^i.

Second, given the admissible velocities, the individual i will select the optimal collision-free velocity which is determined by the given penalty metric. The penalty of a candidate velocity $\boldsymbol{v}_i'$ is defined as

$$penalty(\boldsymbol{v}_i') = w_i \frac{1}{tc_i(\boldsymbol{v}_i')} + \| \tilde{\boldsymbol{v}}_i - \boldsymbol{v}_i' \|,$$

where $\tilde{\boldsymbol{v}}_i$ is the preferred velocity computed from global path planning, w_i is weight, and $tc_i(\boldsymbol{v}_i')$ is the expected collision time. The optimal velocity can be approximated by sampling a number of velocities evenly distributed over admissible velocities. More details can be referred to [16].

Once the collision-free velocity $\boldsymbol{v}_i^{n+1}$ of an individual is obtained, its position is updated by $\boldsymbol{x}_i^{n+1} = \boldsymbol{x}_i^n + \Delta t \boldsymbol{v}_i^{n+1}$.

4) KNOWLEDGE UPDATING

Individual knowledge $\mathcal{K}_i$ is updated according to Equation (1) - (3). The updated individual knowledge is used to construct the path $\mathcal{P}$ in specific knowledge $\mathcal{K}_s$ with the high-level navigation and low-level navigation.

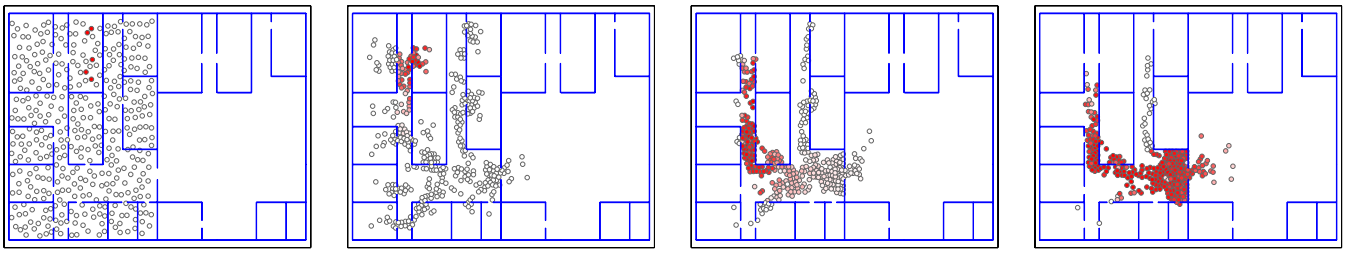

FIGURE 5. Dynamic knowledge transmission in a scenario.

VIII. RESULTS

We evaluate the proposed method with two different scenarios in this section. The motion of the crowd with incomplete knowledge about the two scenarios are computed and analyzed. All reported results were obtained on a machine with a 3.3 GHz Intel Core 2 Duo CPU with 2 GB of RAM.

A. EXPERIMENTAL SETUP

The two scenarios are used in this paper as shown in Fig. 4. In Fig. 4(a), the environment is divided into two subsections c_1 and c_2. In Fig. 4(b), each single room is a subsection. In these scenarios, obstacles are shown as blue lines. In the analysis, the number of individuals in these two scenarios is $N = 400$.

Consider the abilities of expressing knowledge ε_m, assimilating knowledge ϱ_m, and personal influential radius R, we set $\mu_\varepsilon = 0.5$, $\sigma_\varepsilon = 0.2$, $\mu_\varrho = 0.5$, $\sigma_\varrho = 0.2$ and $R = 3$ as the default values in our experiments, unless otherwise specified.

B. ANALYSIS OF KNOWLEDGE TRANSMISSION

We analyze knowledge transmission process in the scenario as shown in Fig. 4(a). In the initial condition, all individuals are located in the c_1 initially and their goals are located in c_2. We assume that the individuals are familiar with c_1 (i.e., $k_i^1 = 1$) but have different familiarity degree with c_2. When these individuals move to subregion c_2, they communicate with their neighbors and obtain knowledge about c_2. Fig. 5 shows the process of dynamic knowledge transmission in the above scenario. In Fig. 5, the circles are individuals, and the colors denote the knowledge k_i^2 about c_2. A darker filled color means a larger individual knowledge. Fig. 5 shows that the knowledge is transmitted to the neighbor individuals gradually, thereby increasing the number of knowledgeable persons in c_2.

Different from previous work [4]–[6], [23], our Personalized-KT model considers the influence of personal factors, such as personal influential radius, knowledge attenuation and disturbance due to personal abilities of expressing and assimilating knowledge etc. To analyze these influential factors, we show the changes of the average number of knowledgeable person $N(k_i^j \geq 0.5)$ over time in Fig. 6. Since many variables are supposed to be subject to different probability distributions, we repeat the experiment 30 times to obtain

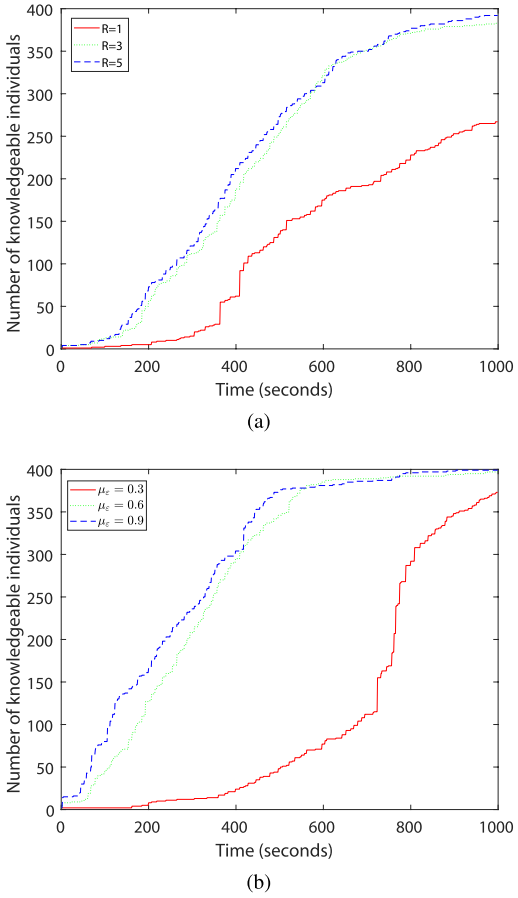

FIGURE 6. The changes of the number of knowledgeable individuals (i.e., $N(k_i^2 > 0.5)$) over time. (a)$N(k_i^2 > 0.5)$ against the personal influential radius R. (b) $N(k_i^2 > 0.5)$ against the μ_ε.

the mean values of $N(k_i^j \geq 0.5)$ for both Fig. 6(a) and Fig. 6(a) respectively. It shows that the number of knowledgeable person increases with an increase in either parameter. Observe that there are some tiny fluctuations because the data is collected during crowd motion process.

As shown in Fig. 6(a), $N(k_i^2 \geq 0.5)$ increases with increasing the personal influential radius R at a given time, but the increase rate progressively slows because the neighbors of the individual will not change even R increases. The main reason is that the sight between the individual and its neighbors may be blocked by the obstacles in the scenario.

Next, we consider how the personal abilities of expressing and assimilating knowledge affect $N(k_i^2 \geq 0.5)$. We adjust the means and standard deviations to obtain different values of ε and ϱ and study their influences on $N(k_i^2 \geq 0.5)$. Fig. 6(b) shows the influence of personal abilities of expressing in the scenario as shown in Fig. 4(a). In this example, we set $R = 3$, $\sigma_\varepsilon = 0.2$, $\mu_\varrho = 0.5$, and $\sigma_\varrho = 0.2$ and gradually varied μ_ε. It shows that the overall number of knowledgeable persons increases with an increase in μ_ε. It means that when people have a higher ability to express knowledge, more people will obtain knowledge faster. Observe that the increase rate also progressively slows with the increase of μ_ε because we only count the number of individuals with $k_i^2 \geq 0.5$, and increasing more on μ_ε contributes little to promoting the increase of $N(k_i^2 \geq 0.5)$. Similar results can also be obtained by varing μ_ϱ.

TABLE 1. The standard deviation of $N(k_i^2 \geq 0.5)$ against the influential radius R and the time window (in seconds).

	0-200	200-400	400-600	600-800	800-1000
R=1	0.65	25.82	22.64	34.49	28.87
R=3	5.98	15.27	11.95	8.31	4.20
R=5	4.31	13.58	9.12	4.76	0.92

Table 1 shows the standard deviation of $N(k_i^2 \geq 0.5)$ against the influential radius R and the time window. Here, we use ϱ_N to denote the standard deviation of $N(k_i^2 \geq 0.5)$. The experimental results show that as R increases, ϱ_N decreases since the knowledge spread faster and much more people obtain the knowledge in a time window. As a result, some influential factors (e.g., uniform distribution of people, etc.) have a smaller impact on the fluctuations of $N(k_i^2 \geq 0.5)$. Thus, the value of ϱ_N reduces. Furthermore, ϱ_N is smaller in the initial and final stages but larger in the intermediate stage given a specific R because $N(k_i^2 \geq 0.5)$ increases slowly in the initial and final stages. Similar conclusion can also be draw when increasing μ_ϱ and μ_ε because the two parameters also determine the knowledge spreading speed as does the influential radius R.

C. ANALYSIS OF KNOWLEDGE-GUIDED WAYFINDING

The Probability-KWF model allows us to produce diverse actions in an unfamiliar environment. We analyze this model by modeling the motion of 10 individuals in the scenario given in Fig. 4(b). In this example, the 10 individuals are uniformly distributed in the office. Fig. 7 shows the routes of the 10 individuals that have different familiarity degree with the subsections (different rooms in this example) in the office. Observe that the result in Fig. 7(a) is only a special case of our method where all individuals are experts. In Fig. 7(b), the two individuals in the upper left of the scenario move to the destination directly because they have already located in their target subregion. Differently, the other individuals search their routes according to their knowledge about the environment. As a result, diverse actions are produced in this process. Evidently, the routes in Figs 7(a) and 7(b) differ greatly, demonstrating that our method considers the difference of individuals and that these individuals tend to take divers actions when having incomplete knowledge of an area.

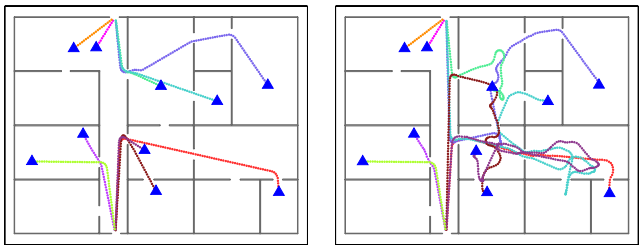

FIGURE 7. The routes (i.e., specific knowledge $\mathcal{K}_S$) of the 10 individuals in the office. The triangles represent the initial positions of the individuals. (a) The routes taken by individuals in method [16]. (b) The routes taken by individuals with incomplete knowledge of the environment in our method.

The Probability-KWF model allows the individuals to adapt to knowledge changes. When individuals obtain more knowledge about the unfamiliar environment, they will have larger opportunities to select the optimal path. We use the heat map of routes to analyze this phenomenon. The heat map is constructed by the density of routes, in which hot colors represent higher route density and cool colors express lower route density. Fig. 8 shows the heat maps of the routes walked by 100 individuals that have different familiarity degree with the scenario. In this example, the 100 individuals are uniform distributed in the scenario shown in Fig.4(b). We suppose the experts are selected from the crowd randomly and the percentage of experts are 0%, 15%, 33%, 67%, and 100%, respectively. The results show that the route distribution is more concentrated when more experts are added to the crowd. For example, in Fig. 8(a), the route distribution is rather dispersed in the red rectangle, while it is rather concentrated in the red rectangle in Fig. 8(e). The reason is that increasing the percentage of experts can speed up knowledge transmission process, making the individual more knowledgeable. These knowledgeable individuals will select shortest path to get their destinations, and thus, the route distribution is more concentrated.

Fig. 7(a) and Fig. 8(e) also show the results of homogeneous crowd simulation methods [1]–[3] which assume that all individuals are familiar with the environment. Observe that it is only a special case of our method where all individuals are experts as shown in Fig. 7(a) and Fig. 8(e). Thus, the proposed method can simulate heterogeneous crowd evacuation in various situations flexibly by setting different parameters.

We future evaluate the proposed method on real-world situations by comparing the results with the two discoveries obtained from the real-world experiment in [31]. The real-world experiment is about way finding behaviors of participants which consist of 24 novices and 28 experts in a library. There are two meaningful discoveries in the real-world experiment. First, participants with familiarity walk shorter extra distance than do participants with no familiarity in all

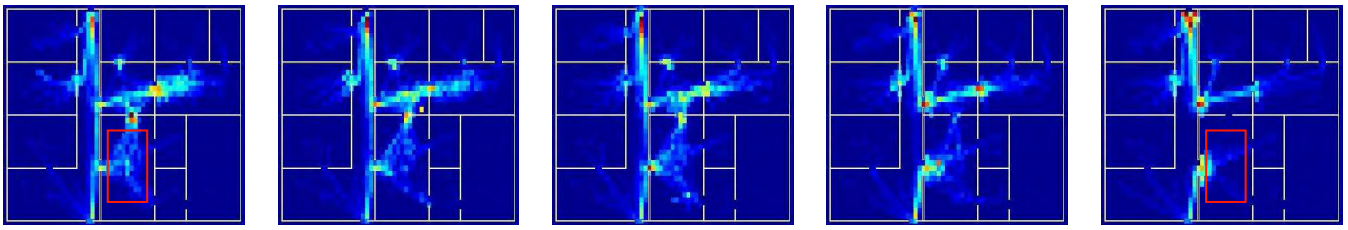

FIGURE 8. Heat maps of routes walked by the crowd that has different familiarity with the environment. From (a) to (e): the experts are selected from the crowd randomly and the percentage of experts are 0%, 15%, 33%, 67%, and 100%, respectively. The method [16] that assumes all individuals are familiar with the environment only obtains the heat map in (e).

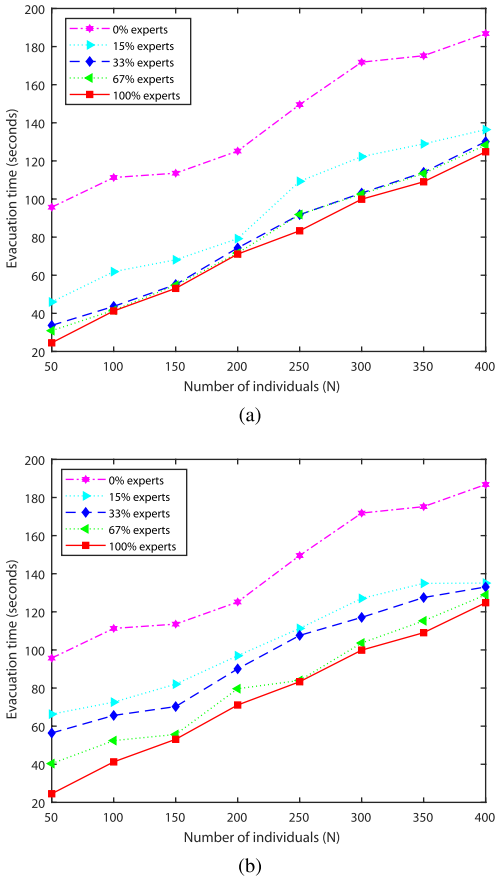

FIGURE 9. Average timing statistics for crowd evacuation with different population size and familiarity degree. (a) The personal influential radius is set to $R = 2$. (b) The personal influential radius is set to $R = 1$.

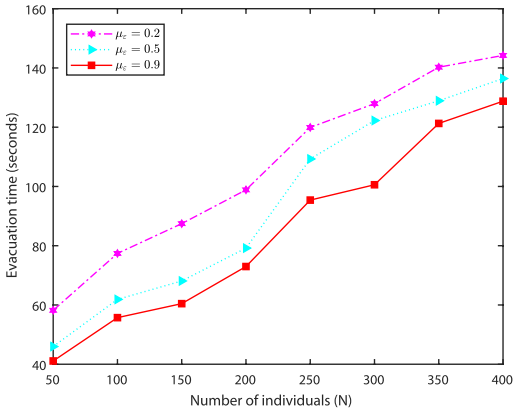

FIGURE 10. Average timing statistics for crowd evacuation with different population size and μ_ε.

locations. Second, novices' routes cover larger areas on all the floors. As shown in Fig. 7(b)-(d), individuals with incomplete knowledge take diverse individual paths which are much longer than the shortest paths taken by experts in Fig. 7(a). Thus, the result is agreed with the first discovery. As shown in Fig. 8(a), the heat map of routes is more dispersed than that in Fig. 8(e). So, the novices' routes cover larger areas and the result is consistent with the second discovery.

D. CROWD EVACUATION IN AN UNFAMILIAR ENVIRONMENT

Fig. 9 and Fig. 10 show the average timing statistics for crowd evacuation in the scenario as shown in Fig. 4(b). The experiment is repeated 30 times for collecting the mean values of evacuation time for both Fig. 9 and Fig. 10 respectively. In this example, the size of the office is 31 $m \times 21$ m and the evacuation time for the 8 groups of people with different size and different number of experts is shown in Fig. 9. Results show that when the crowd has more knowledge, the evacuation takes less time, regardless of congestion. For example, the crowd that has 100% experts has the least evacuation time, whereas the crowd that has 0% experts take the longest time to finish. When the ratio of experts is increased, more individuals have chances to receive knowledge, thereby reducing the evacuation time.

Fig. 9 also shows the impacts of different personal influential radius on evacuation time. In Fig. 9(a) and (b), R is set to $R = 2$ and $R = 1$ respectively. It shows that when R decreases, the evacuation time increases accordingly because speed of knowledge transmission is reduced and less neighbors can receive the knowledge at a time. Furthermore, the effect of R on evacuation time is reduced when crowd density increases. As shown in Fig. 9, when the number of the individuals increases to 400, the evacuation time of different cases is considerably close to each other. The reason is that increasing R contributes little to promoting knowledge transmission since the sight between individuals are blocked by obstacles in the scenario, and the number of neighborhood individuals will not change much.

Fig. 10 shows the evocation time with different population size and knowledge expression ability μ_ε. In this experiment,

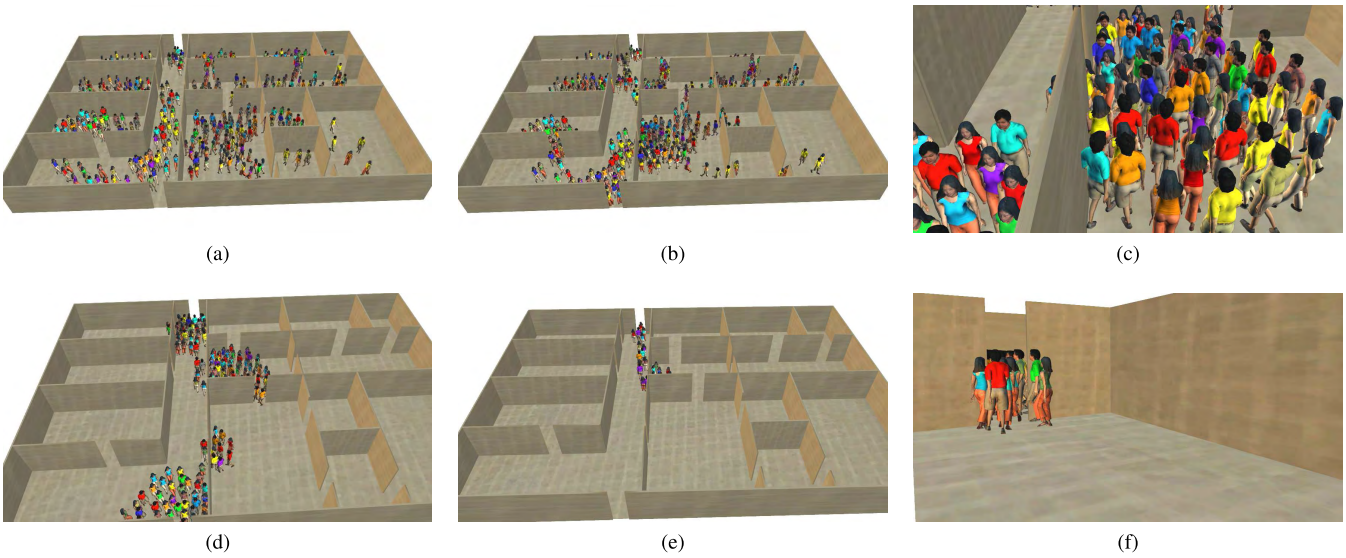

FIGURE 11. A sequence of crowd simulation results in our system.

the values of μ_ε is adjusted, whereas the other parameters are default values. The results demonstrate that larger value of μ_ε leads to less evocation time, because increasing the abilities of expressing knowledge produces less knowledge attenuation and disturbance.

TABLE 2. The standard deviation of evacuation time ϱ_T (in seconds) against the different population size N and the familiarity degree $\mathcal{K}$.

	50	100	150	200	250	300	350	400
0%	16.82	12.71	10.11	8.78	7.39	6.50	5.17	4.86
15%	13.98	10.67	8.85	7.45	6.41	5.37	4.58	4.15
33%	11.64	8.56	7.32	6.67	5.93	4.69	4.06	3.97
67%	7.91	6.89	6.29	5.22	4.57	3.84	3.52	3.46
100%	6.27	5.95	5.63	4.49	4.33	3.26	2.80	2.54

Table 2 shows the standard deviation of the evacuation time ϱ_T against the different population size N and familiarity degree $\mathcal{K}$. The experimental results show that as the percentage of expert increases, $\mathcal{K}$ increases, and ϱ_T decreases. The reason is that more people have enough knowledge to select a definite optimal path when increasing $\mathcal{K}$, and the uncertain time of path exploration have a smaller influence on the evacuation time. Therefore, ϱ_T is reduced. Conversely, the influence of the uncertain time for path exploration increases with a decreasing number of experts, and thus ϱ_T increases. In addition, ϱ_T decreases when N increases because the influence of the uniformly distributed people positions is reduced. Similarly, ϱ_T also decreases with an increase in both μ_ε and μ_ϱ since knowledge is spread faster in these conditions. Thus, the uncertain exploration time is reduced accordingly.

E. VISUALIZE THE CROWD MOTION

A 3D crowd simulation system is designed to compute crowd motion and exhibit the final simulation results. Our system adopts Microsoft .NET Framework 4.5.1, Visual Studio 2013 and Microsoft XNA Game Studio 4.0 for developing the real-time crowd simulation framework. To achieve 3D realistic crowd simulation results, we create a large numbers of photo-realistic human models with scanning techniques provided by Microsoft Kinect. In addition, the motion (i.e.,walk, run, etc.) of these models are driven by motion capture data, which are available from CMU (Carnegie Mellon University) motion capture data base at http://mocap.cs.cmu.edu/search.php?subjectnumber=2&trinum=1. The trajectories of crowd motion are computed by the proposed method in this paper.

Fig. 11 shows a sequence of the crowd simulation results. In this example, 400 individuals attempt to move to the two exits of the office. Both the close-up and far-away images are provided to demonstrate the evacuation process intuitively. Images show that our system can exhibit the cultural and social behavior during evacuation process in a high degree of visual realism. Provide such an intuitive tool is beneficial, because the results can be accepted and understood by non-professionals and decision-makers more easily.

IX. CONCLUSION

Crowd simulation in an unfamiliar environment is a major consideration especially for safety evacuation. Crowd behavior in an unfamiliar environment is influenced by many factors (e.g., personal influential radius, knowledge attenuation and disturbance due to personal abilities of expressing and assimilating knowledge, etc.). Thus, modeling crowd motion that has incomplete knowledge of the environment presents a challenging issue. We propose a framework for computing the actual human behaviors in an unfamiliar environment. The framework quantifies and analyzes the above factors by defining three predominant procedures: knowledge representation, dynamic knowledge transmission and knowledge-guided wayfinding. In these procedures, we design the

Semantic-LS to represent knowledge about the unfamiliar environment, construct the Personalized-KT model to capture important influential factors for knowledge transmission, and present a Probability-KWF model to produce diverse actions and allow the individuals to adapt to knowledge changes in an unfamiliar environment.

Our framework provides flexible and controllable modeling tools for crowd motion. A simulation system is also implemented to visualize the analysis in a graphical manner. This method can be applied to emergency response management for safety accidents. We would like extend our method to consider human reasoning in the mental world during wayfinding process in our future work. Furthermore, although the Semantic-LS represent the knowledge about the environment intuitively, it is complex for some situations, especially for large interior scenarios that involve many obstacles and have no obvious boundaries (e.g., a big clothing department store with many clothing booths). In the future, we would like to design more effective knowledge representation method for such complex situations. In addition, extending our method to consider crowd evacuation in multilayer building as introduced in [14] is also challenging and interesting.

REFERENCES

[1] W. G. V. Toll, A. F. Cook, IV, and R. Geraerts, "Real-time density-based crowd simulation," *Comput. Animation Virtual Worlds*, vol. 23, no. 1, pp. 59–69, 2012.
[2] L. Hoyet, A. H. Olivier, R. Kulpa, and J. Pettré, "Perceptual effect of shoulder motions on crowd animations," *ACM Trans. Graph.*, vol. 35, no. 4, pp. 53-1–53-10, 2016.
[3] H. Liu, B. Xu, D. Lu, and G. Zhang, "A path planning approach for crowd evacuation in buildings based on improved artificial bee colony algorithm," *Appl. Soft Comput.*, vol. 68, pp. 360–376, Jul. 2018.
[4] J. Tsai *et al.*, "ESCAPES—Evacuation simulation with children, authorities, parents, emotions,and social comparison," in *Proc. 10th Int. Conf. Auto. Agents Multiagent Syst. (AAMAS)*, 2011, pp. 457–464.
[5] N. Pelechano and N. I. Badler, "Modeling crowd and trained leader behavior during building evacuation," *IEEE Comput. Graph. Appl.*, vol. 26, no. 6, pp. 80–86, Nov./Dec. 2006.
[6] H. Liu, B. Liu, H. Zhang, L. Li, X. Qin, and G. Zhang, "Crowd evacuation simulation approach based on navigation knowledge and two-layer control mechanism," *Inf. Sci.*, vols. 436–437, pp. 247–267, Apr. 2018.
[7] C. W. Reynolds, "Flocks, herds and schools: A distributed behavioral model," *ACM SIGGRAPH Comput. Graph.*, vol. 21, no. 4, pp. 25–34, Jul. 1987.
[8] D. Helbing and P. Molnár, "Social force model for pedestrian dynamics," *Phys. Rev. E, Stat. Phys. Plasmas Fluids Relat. Interdiscip. Top.*, vol. 51, no. 5, p. 4282, 1995.
[9] S. Mohamad *et al.*, "Making decision for the next step in dense crowd simulation using support vector machines," in *Proc. ACM SIGGRAPH Conf. Virtual-Reality Continuum Appl. Ind.*, 2016, pp. 281–287.
[10] H. Liu, Y. Sun, and Y. Li, "Modeling and path generation approaches for crowd simulation based on computational intelligence," *Chin. J. Electron.*, vol. 21, no. 4, pp. 636–641, 2012.
[11] A. Golas, R. Narain, S. Curtis, and M. C. Lin, "Hybrid long-range collision avoidance for crowd simulation," *IEEE Trans. Vis. Comput. Graphics*, vol. 20, no. 7, pp. 1022–1034, Jul. 2014.
[12] A. Sud, R. Gayle, and E. Andersen, "Real-time navigation of independent agents using adaptive roadmaps," in *Proc. ACM Symp. Virtual Reality Softw. Technol.*, 2007, pp. 99–106.
[13] A. Treuille, S. Cooper, and Z. Popović, "Continuum crowds," *ACM Trans. Graph.*, vol. 25, no. 3, pp. 1160–1168, 2006.
[14] H. Jiang, W. Xu, T. Mao, C. Li, S. Xia, and Z. Wang, "Continuum crowd simulation in complex environments," *Comput. Graph.*, vol. 34, no. 5, pp. 537–544, 2010.
[15] S. Patil, J. van den Berg, S. Curtis, M. C. Lin, and D. Manocha, "Directing crowd simulations using navigation fields," *IEEE Trans. Vis. Comput. Graphics*, vol. 17, no. 2, pp. 244–254, Feb. 2011.
[16] J. van den Berg, M. Lin, and D. Manocha, "Reciprocal velocity obstacles for real-time multi-agent navigation," in *Proc. IEEE Int. Conf. Robot. Autom.*, May 2008, pp. 1928–1935.
[17] R. Kulpa, A. H. Olivierxs, A. H. Olivierxs, J. OndYej, and J. Pettré, "Imperceptible relaxation of collision avoidance constraints in virtual crowds," *ACM Trans. Graph.*, vol. 30, no. 6, p. 138, 2011.
[18] G. Zhang, D. Lu, and H. Liu, "Strategies to utilize the positive emotional contagion optimally in crowd evacuation," *IEEE Trans. Affect. Comput.*, May 2018, doi: 10.1109/TAFFC.2018.2836462
[19] M. Cao, G. Zhang, M. Wang, D. Lu, and H. Liu, "A method of emotion contagion for crowd evacuation," *Phys. A, Stat. Mech. Appl.*, vol. 483, pp. 250–258, Oct. 2017.
[20] H. Liu, Y. Li, W. Li, and G. Zhang, "A grouping approach based on non-uniform binary grid partitioning for crowd evacuation simulation," *Concurrency Comput. Pract., Exper.*, Mar. 2018, doi: doi.org/10.1002/cpe.4493.
[21] D. Lu, X. Huang, G. Zhang, X. Zheng, and H. Liu, "Trusted device-to-device based heterogeneous cellular networks: A new framework for connectivity optimization," *IEEE Trans. Veh. Technol.*, vol. 67, no. 11, pp. 11219–11233, Nov. 2018.
[22] Z. Zhao, Y. Zhang, C. Li, L. Ning, and J. Fan, "A system to manage and mine microblogging data," *J. Intell. Fuzzy Syst.*, vol. 33, no. 1, pp. 315–325, 2017.
[23] Y. Han and H. Liu, "Modified social force model based on information transmission toward crowd evacuation simulation," *Phys. A, Stat. Mech. Appl.*, vol. 469, pp. 499–509, Mar. 2017.
[24] A. Golas, R. Narain, and M. Lin, "Continuum modeling of crowd turbulence," *Phys. Rev. E, Stat. Phys. Plasmas Fluids Relat. Interdiscip. Top.*, vol. 90, no. 4, p. 042816, 2014.
[25] L. C. Mei, P. Parigi, K. Law, and J. C. Latombe, "A computational framework incorporating human and social behaviors for occupant-centric egress simulation," Stanford Univ., Stanford, CA, USA, Tech. Rep. TR219, 2015. [Online]. Available: http://minoe.stanford.edu/publications/zan_chu/CIFE2015.pdf
[26] C. Cocking, J. Drury, and S. Reicher, "The psychology of crowd behaviour in emergency evacuations: Results from two interview studies and implications for the fire and rescue services," *Irish J. Psychol.*, vol. 30, nos. 1–2, pp. 59–73, 2009.
[27] M. Sung, L. Kovar, and M. Gleicher, "Fast and accurate goal-directed motion synthesis for crowds," in *Proc. ACM SIGGRAPH/Eurograph. Symp. Comput. Animation*, 2005, pp. 291–300.
[28] A. Lipowski and D. Lipowska, "Roulette-wheel selection via stochastic acceptance," *Phys. A, Statist. Mech. Appl.*, vol. 391, no. 6, pp. 2193–2196, 2012.
[29] C. Hu, H. Liu, and P. Zhang, "Cooperative co-evolutionary artificial bee colony algorithm based on hierarchical communication model," *Chin. J. Electron.*, vol. 25, no. 3, pp. 570–576, 2016.
[30] P. Zhang, H. Liu, and Y. Ding, "Dynamic bee colony algorithm based on multi-species co-evolution," *Appl. Intell.*, vol. 40, no. 3, pp. 427–440, 2014.
[31] R. Li and A. Klippel, "Wayfinding behaviors in complex buildings: The impact of environmental legibility and familiarity," *Environ. Behav.*, vol. 48, no. 3, pp. 482–510, 2016.

GUIJUAN ZHANG received the Ph.D. degree from the Institute of Computing Technology (ICT), Chinese Academy of Sciences, in 2011. She is currently an Associate Professor at the School of Information Science and Engineering, Shandong Normal University, China. Her current research interests include affective computing and computer simulation.

DIANJIE LU received the Ph.D. degree from the Institute of Computing Technology, Chinese Academy of Sciences, in 2012. He is currently an Associate Professor with the School of Information Science and Engineering, Shandong Normal University, China. His current research interests include affective computing, resource allocation, and routing in cognitive radio networks.

LEI LV received the Ph.D. degree from the Institute of Computing Technology, Chinese Academy of Sciences. He is currently an Assistant Professor with the School of Information Science and Engineering, Shandong Normal University, China. His current research interests include crowd simulation and virtual reality.

HUI YU received the Ph.D. degree in computer science from the Institute of Computing Technology, Chinese Academy of Sciences. She is currently an Assistant Professor with the School of Management Science and Engineering, Shandong Normal University. Her research interests include natural language processing and machine translation.

HONG LIU received the Ph.D. degree from the Institute of Computing Technology, Chinese Academy of Sciences, in 1998. She is currently a Professor of computer science with the School of Information Science and Engineering, Shandong Normal University, China. Her research interests include pervasive computing, computer-aided design, multi-agent systems, and cooperative design.